Reprint Series
25 January 1985, Volume 227, pp. 411–413

SCIENCE

Highly Supercooled Cirrus Cloud Water: Confirmation and Climatic Implications

Kenneth Sassen, Kuo Nan Liou, Stefan Kinne, and Michael Griffin

Highly Supercooled Cirrus Cloud Water: Confirmation and Climatic Implications

Abstract. *Liquid cloud droplets supercooled to temperatures approaching −40°C have been detected at the base of a cirrostratus cloud through a combination of ground-based, polarization laser radar (lidar) and in situ aircraft measurements. Solar and thermal infrared radiative budget calculations based on these observations indicate that significant changes in the atmospheric heating distribution and the surface radiative budget may be attributed to liquid layers in cirrus clouds.*

The meteorological classification of atmospheric clouds is based on the mechanism of cloud formation, as reflected in their appearance and spatial structure, and these cloud categories are then subdivided according to cloud altitude. Since temperatures decrease steadily with height in the troposphere, this grouping into low, middle, and high clouds is pertinent to the thermodynamic phase of the clouds under standard atmospheric conditions. Although water droplets can exist at temperatures well below 0°C, the probability that a supercooled cloud will glaciate increases rapidly with decreasing temperature. If cloud droplets are composed of pure water, a small drop will likely remain in a supercooled state until its temperature approaches the spontaneous freezing point of water, about −40°C, before homogeneous nucleation occurs (*1*). However, special particles, or ice nuclei, that are capable of initiating heterogeneous nucleation at much warmer temperatures are usually present in the atmosphere. Measurements of natural ice nuclei in the lower atmosphere show a strong temperature dependence. Particles that are active at temperatures warmer than about −10°C are relatively scarce, but with decreasing temperatures the concentrations of ice nuclei increase exponentially (*2*).

Since the family of cirrus clouds occurs in the upper troposphere, even extending to the tropopause where temperatures are extremely cold (−50° to −60°C), cirrus clouds are commonly thought to be composed of ice crystals. Indeed, it seems implicit in the definition of cirrus clouds that liquid water, in any measurable amounts, should be absent. Recent evidence provided by remote sensing observations, however, would indicate that cloud liquid water can exist in a highly supercooled state within the temperature range typical of at least the lower cloud regions of cirrus clouds (*3–5*). To account for these observations, it has been suggested that impurities from hygroscopic cloud condensation nuclei, such as ammonium sulfate, depress the homogeneous freezing temperature (*3*) and that ice nuclei derived from the earth's surface are uncommon at such great altitudes (*4*).

A field research program, designed in part to test the hypothesis that highly supercooled water can be present in cirrus clouds and can play a significant role in their formation and radiative properties, was recently carried out in the vicinity of the Colorado Front Range near Boulder, Colorado. Measurements were made with a ground-based ruby lidar system (*6*), and a specially instrumented jet aircraft designed to provide in situ measurements of cirrus cloud content was used. The Sabreliner research aircraft of the National Center for Atmospheric Research (NCAR) was equipped with a number of probes to measure the sizes and concentrations of both ice crystals and cloud droplets and to routinely record other pertinent information such as the upward and downward fluxes of solar and terrestrial radiation (*7*). With the polarization technique used by the lidar, cloud droplets can be discriminated from ice crystals through the use of the linear depolarization ratio δ, defined as the ratio of the backscattered laser power in the plane of polarization orthogonal to the linearly polarized source divided by the backscattered laser power in the plane of polarization parallel to the source. This capability is a consequence of the principle that spherical particles (for example, cloud droplets) do not depolarize the incident electromagnetic waves during single scattering, whereas nonspherical scatterers such as ice crystals introduce a depolarized component into the backscattering.

Verification of the presence of highly supercooled cirrus cloud water was obtained from an approximately 2-km-thick, layered cirrostratus cloud on 17 October 1983. The lidar returns indicated a liquid cloud signature at the 8.5-km base (above mean sea level) of the cirrus layer at 1735 G.M.T. (Fig. 1). The aircraft was subsequently directed to sam-

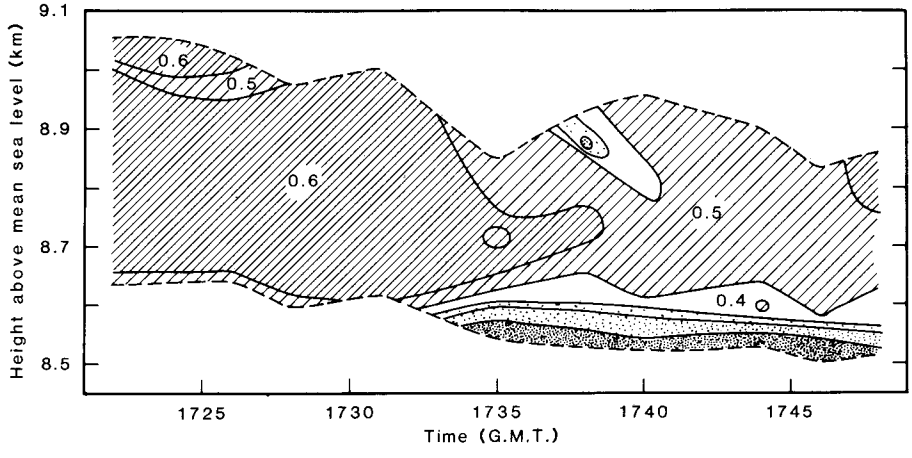

Fig. 1. Height versus time display of linear depolarization ratios generated from vertically pointing lidar measurements during the initial appearance of highly supercooled liquid water at the bottom of a 2-km-thick cirrostratus cloud on 17 October 1983. A gradual water-to-ice cloud transformation is shown by the decreasing stippling just above the cloud base. The cloud boundaries (dashed lines) derived from the δ value analysis often do not correspond to the actual cloud boundaries, particularly in the presence of significant optical attenuation.

ple the cloud base at a heading corresponding to the direction of a lidar elevation-angle scan. Figure 2 depicts the remote and in situ data from these coordinated observations. In Figs. 1 and 2 lidar δ value isopleths for the lower cloud region are shown with the average δ value in each characteristically shaded interval. The lightly cross-hatched areas ($\delta = 0.5 \pm 0.05$) are typical of pure ice clouds, and the $\delta \leq 0.05$ values shown by the solid areas correspond to a nearly pure water cloud. Intermediate values represent a mixed water- and ice-phase environment, and the gradient in δ values with height above the cloud base indicates a gradual transformation of cloud particles from the liquid to solid phase (*8*). Note, in Fig. 1, the alteration in ice cloud δ values with the appearance of the liquid bottom layer, implying a change in ice crystal shape.

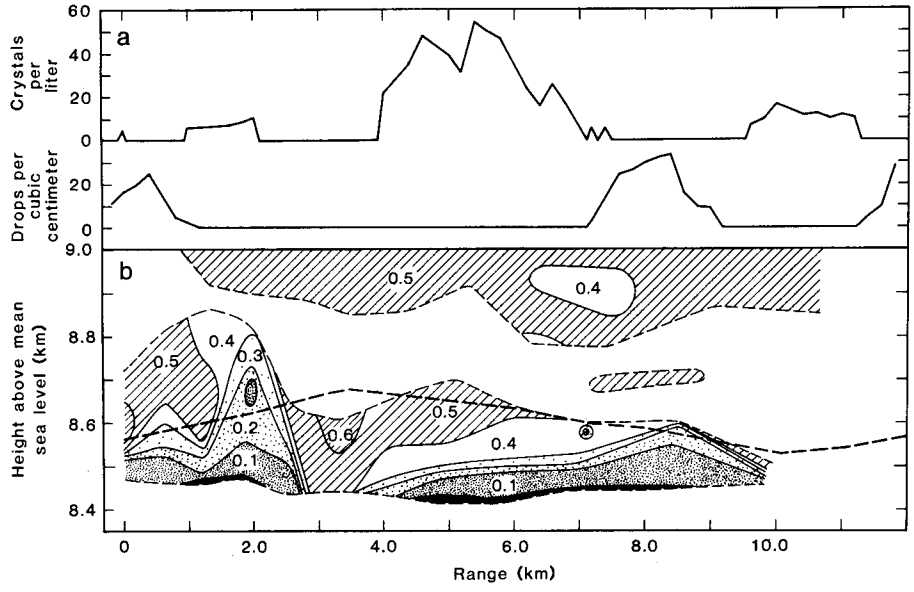

Fig. 2. (a) In situ data for cloud droplets per cubic centimeter and ice crystals per liter. (b) Range versus height display of lidar δ values derived from a 90° to 30° scan of the elevation angle, showing the gradual freezing of cloud droplets above the cirrostratus cloud base. The position of the aircraft relative to the cloud is shown by the heavy dashed line.

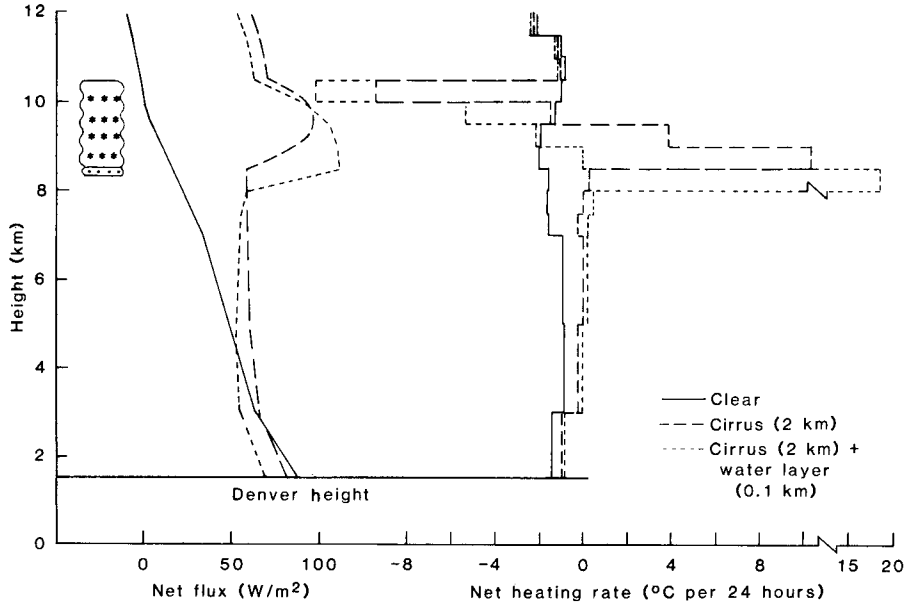

Fig. 3. Radiative heating rate profiles for clear and cloudy atmospheres containing a 2-km-thick cirrus cloud, with and without a 100-m-thick water layer at the cloud base. We obtained the net fluxes by adding the net solar and infrared fluxes; we derived the net heating rates from the net flux divergence, assuming a motionless atmosphere. A solar constant of 1360 W/m^2, a surface albedo of 20 percent, and a sunlight duration of 12 hours were used in the computations, along with temperature and humidity profiles obtained from upper-air sounding data from nearby Denver, Colorado. The ice and liquid water contents of the clouds were 0.011 and 0.06 g/m^3, respectively.

The lidar and aircraft data collected during the period of coordinated measurements (Fig. 2) are generally in agreement (*9*). An in situ probe detected peak concentrations of 25 to 35 drops per cubic centimeter (mean diameter, 5 μm) in cloud regions shown by the lidar to be of mixed phase composition (*10*). The ice crystals in these regions were probably too small to be detected by the airborne ice crystal probe, but minute crystals with dimensions of ~50 μm were measured higher above the cloud base. Although the aircraft did not penetrate the cloud base areas corresponding to the lowest δ values in this part of the flight leg, from 100 to 130 drops per cubic centimeter were measured at a range of 15 to 18.5 km. According to the aircraft records, liquid water was measured at temperatures between −35° and −36°C. In comparison with earlier reported aircraft measurements, the detection of such highly supercooled water is unique.

In recent years there has been growing interest in the effects of cirrus clouds on the earth's climate and climatic changes. Various climate models have illustrated that cirrus clouds can profoundly affect the transfer of solar and terrestrial radiation fluxes through the atmosphere and thereby influence the temperature structure of the earth-atmosphere system (*11*). In these models it was assumed that the ice crystals had simple shapes and that the clouds were composed entirely of ice crystals. However, modifications in the radiation balance caused by the presence of liquid droplets in cirrus clouds, and the related changes in the shapes of ice crystals nucleated from them, have not, to our knowledge, received attention.

In order to investigate the possible climatic effects of highly supercooled liquid water in cirrus clouds, we have carried out radiative budget calculations based on the mean cloud contents observed by the aircraft. The calculations involved the transfer of both solar and thermal infrared radiation through the simulated cloudy atmosphere, and our earlier programs (*12*) were modified so that the internal fluxes in 500-m-thick layers within the cloud could be evaluated. To examine the effects of a thin water layer on the radiative budget, vertical flux distributions were computed with and without the insertion of a 100-m-thick water layer into the model at the bottom of a 2-km-thick cirrus cloud. Mie scattering calculations for particle size distributions similar to those measured were performed to obtain the single scattering parameters. Corrections to adjust for the nonspherical shape of hexagonal

ice crystals were based on detailed scattering phase functions and extinction and scattering cross sections and were applied at selected wavelengths in the solar and infrared spectra (*13*).

Figure 3 depicts the net flux and heating rate (per 24-hour interval) profiles for these two cloud models. The results for a cloudless atmosphere are presented for comparison. With regard to the atmospheric heating rates of the pure-ice cirrus cloud, a significant cooling at the cloud top (~9°C per 24 hours) and a pronounced warming at the cloud base (~10°C per 24 hours) are apparent. With the insertion of the 100-m-thick bottom-water layer into the model, the cooling rate is enhanced by about 3°C per 24 hours at the cirrus cloud top. Of more importance, however, is the greenhouse effect caused by an almost twofold increase in the atmospheric heating rate at the cloud base. With respect to the net flux, the thin water layer reduced the net flux available at the surface, the dominant factor determining the surface temperature, by ~12 W (about 15 percent) as compared to the pure ice cloud.

It follows from these relatively simple calculations that, when compared to pure-ice clouds, water-containing cirrus clouds can significantly enhance the atmospheric warming between the surface and the cloud base and, at the same time, can produce a cooling of the surface from the reduced downward solar flux. Although in these exercises we assumed that the cirrus clouds persisted for the 24-hour period over which the net heating rate calculations were averaged, it should be acknowledged that our measurements were insufficient to characterize the cloud layer over such a time scale. Nonetheless, it is clear that the presence of even a thin water layer at the cirrus cloud base will modify the fundamental radiative properties of the cloud, most notably the infrared emissivity and the solar albedo, and will therefore have an impact on attempts to model the climate of the earth-atmosphere system. To aid in the determination of the requisite cloud microphysical inputs for future climate models, it is of paramount importance to obtain climatological data on the frequency and distribution of liquid water within cirrus clouds. It would appear from the findings reported here that ground-based observation programs can be used to provide this information.

KENNETH SASSEN
KUO NAN LIOU
STEFAN KINNE
MICHAEL GRIFFIN
Department of Meteorology, University of Utah, Salt Lake City 84112

References and Notes

1. P. V. Hobbs, *Ice Physics* (Clarendon, Oxford, 1974), p. 461; D. E. Hagen, R. J. Anderson, J. L. Kassner, Jr., *J. Atmos. Sci.* **38**, 1236 (1981).
2. H. R. Pruppacher and J. D. Klett, *Microphysics of Clouds and Precipitation* (Reidel, Boston, 1978), p. 241.
3. R. J. Curran and M. C. Wu, *J. Atmos. Sci.* **39**, 635 (1982).
4. K. Sassen, *J. Climate Appl. Meteorol.* **23**, 568 (1984).
5. A significant change in lidar-measured high-cloud scattering properties was reported to occur at a temperature of −40°C by C. M. R. Platt and A. C. Dilley [*J. Atmos. Sci.* **38**, 1069 (1981)]. More recently, A. J. Heymsfield and C. M. R. Platt [*ibid.* **41**, 846 (1984)] have indicated that small supercooled drops could have contributed significantly to these changes.
6. The ruby laser has a wavelength of 0.694 μm; see Sassen (*4*) for a description of the lidar system.
7. For an example of the application of airborne radiometric measurements for the determination of the radiative properties of cirrus clouds, see K. T. Griffith, S. K. Cox, R. G. Knollenberg, *J. Atmos. Sci.* **37**, 1077 (1980).
8. This interpretation of the gradient in δ values is based on laboratory laser-scattering measurements of artificially "seeded" supercooled water clouds, which demonstrate that frozen cloud droplets are sufficiently nonspherical in shape to provide an ice cloud depolarization signature within 5 to 15 seconds after freezing [K. Sassen and K. N. Liou, *J. Atmos. Sci.* **36**, 852 (1979)].
9. A review of the airborne techniques used for probing cloud microstructure is given by R. G. Knollenberg, in *Clouds: Their Formation, Optical Properties, and Effects*, P. V. Hobbs and A. Deepak, Eds. (Academic Press, New York, 1981), p. 15. The in situ data of Fig. 2 were derived from measurements made with the forward scattering spectrometer probe (FSSP, for cloud droplets) and the two-dimensional ice crystal probe. Although the response of the FSSP to newly frozen cloud droplets is uncertain, an additional in situ probe, the Rosemont icing-rate detector, collected independent data supporting identification of supercooled water.
10. The mixed-phase cloud area centered at a range of 2 km in Fig. 2 resembles a convective cell pattern. Since the aircraft encountered only minute ice crystals at this location about 2 minutes after the lidar scan was performed, it is possible that this portion of the cloud became glaciated in the interim.
11. K. N. Liou and K. L. Gebhart, *J. Meterol. Soc. Jpn.* **60**, 570 (1982); S. C. S. Ou and K. N. Liou, *J. Atmos. Sci.*, **41**, 2289 (1984).
12. K. N. Liou and S. C. S. Ou, *J. Atmos. Sci.* **40**, 214 (1983).
13. Q. Cai and K. N. Liou, *Appl. Opt.* **21**, 3569 (1982).
14. We thank K. T. Griffith and other members of the staff of the NCAR Research Aviation Facility for their efforts in obtaining and analyzing the aircraft data. This research was supported by NSF grant ATM82-10709. NCAR is sponsored by the National Science Foundation.

6 August 1984; accepted 25 October 1984